Translational Oncology
www.transonc.com

Volume 8 Number 3 June 2015 pp. 163–168 163

The Value of Proton Magnetic Resonance Spectroscopy in High-Intensity Focused Ultrasound Treatment of Experimental Liver Cancer[1]

Zhuo-yue Tang*†, Jian-nong Zhao*, Wei-jia Zhong*, Yin-deng Luo*, Wei Wu*, Wei-juan Chen* and Yu-bing Dai‡

*Department of Radiology, The Second Affiliated Hospital of Chongqing Medical University, Chongqing, China; †Department of Radiology, Chongqing People's Hospital, Chongqing, China; ‡Department of Otolaryngology, Guizhou Provincial People's Hospital, Guiyang, China

Abstract

High-intensity focused ultrasound (HIFU) is a rapidly developing, non-invasive technique for local treatment of solid tumors that produce coagulative tumor necrosis. This study is aimed to investigate the feasibility of proton magnetic resonance spectroscopy (MRS) on early assessing treatment of HIFU ablation in rabbit with VX2 liver tumor. HIFU ablation was performed on normal liver and VX2 tumor in rabbit, and MRS was performed on normal liver and VX2 tumor before and 2 days after 100% HIFU ablation or 80% ablation in tumor volume. Choline (Cho) and choline/lipid (Cho/Lip) ratios between complete and partial HIFU ablation of tumor were compared. Tissues were harvested and sequentially sliced to confirm the necrosis. In normal liver, the Cho value liver was not obviously changed after HIFU ($P > .05$), but the Cho/Lip ratio was decreased ($P < .05$). Cho in liver VX2 tumor was much higher than that in normal liver ($P < .001$). Cho and Cho/Lip ratio were significantly decreased in tumor after complete HIFU ablation and partial HIFU ablation, and the Cho value in complete HIFU tumor ablation did not show any difference from that in normal liver after HIFU ($P > .05$); however, the Cho value in partial ablation was still higher than that in normal liver before or in tumor after complete HIFU treatment due to the residual part of tumors, and Cho/Lip ratio is lower than that in complete HIFU treatment ($P < .001$). The changes in MRS parameters were consistent with histopathologic changes of the tumor tissues after treatment. MRS could differentiate the complete tumor necrosis from residual tumor tissue, when combined with magnetic resonance imaging. We conclude that MRS may be applied as an important, non-invasive biomarker for monitoring the thoroughness of HIFU ablation.

Translational Oncology (2015) 8, 163–168

Introduction

High-intensity focused ultrasound (HIFU) is a rapidly developing, non-invasive technique for local treatment of solid malignancies that can produce coagulative tumor necrosis and destroy tumor blood vessels at a precise focal point, without harming overlying and adjacent structures even within the path of the beam [1,2].

Recent clinical trials showed favorable outcomes of HIFU ablation in liver cancer, which can be used as a viable, non-invasive cancer ablation approach, especially for intermediate to advanced stage liver cancer [3]. The success of HIFU treatment relies on complete coagulative tumor necrosis after HIFU ablation. The verification of completeness of coagulative tumor necrosis immediately or early after HIFU ablation is still a challenge for clinical oncologists, and the treatment monitoring

Address all correspondence to: Jian-nong Zhao, MD, Department of Radiology, The Second Affiliated Hospital of Chongqing Medical University, Chongqing 400010, China. E-mail: jiannong_zhao@sina.cn

[1] This study was supported by the National Natural Science Foundation of China (grant 30800262) and the Medical Research Key Program of the National Health and Family Planning Commission of Chongqing, China (grant 20141016). Declaration of conflict of interest: None.
Received 8 January 2015; Revised 25 March 2015; Accepted 30 March 2015

© 2015 The Authors. Published by Elsevier Inc. on behalf of Neoplasia Press, Inc. This is an open access article under the CC BY-NC-ND license (http://creativecommons.org/licenses/by-nc-nd/4.0/).

1936-5233/15
http://dx.doi.org/10.1016/j.tranon.2015.03.007

and evaluation cannot be only made reliably by conventional imaging techniques. Therefore, the utility of appropriate imaging method, which can accurately and timely evaluate the completeness of tumor necrosis after HIFU treatment, will have very important clinical significance [3,4]. On timely detection, any residual tumor may regain the chance of eradication through a complementary treatment during the initial or early after HIFU ablation.

Magnetic resonance spectroscopy (MRS) can qualify intracellular biochemical and metabolite concentration *in vivo* as a non-invasive means for the characterization of tissue and pathophysiological changes, which is used to aid in diagnosis in tumors as well as to monitor the cancer treatment response. Clinical studies also showed the value of MRS for the differentiation of recurrent or residual brain tumor activity from surrounding healthy tissue and necrotic tumor processes [4,5]. MRS has been used to evaluate the focal hepatic lesions and the early stage metabolic changes of hepatocellular carcinoma after transcatheter arterial chemoembolization [6]. Therefore, MRS may have the potential to evaluate coagulative tumor necrosis *in vivo* after HIFU ablation. The aim of this study is to investigate the possibility of MRS as a non-invasive technique to differentiate the complete coagulative tumor necrosis from residual tumor tissue. Herein, we conducted the study to examine MRS change in normal liver after HIFU ablation and the differences of MRS in distinct extent of coagulative necrosis of HIFU-ablated VX2 liver tumor followed by subsequent histologic documentation.

We found that choline (Cho) compounds and choline/lipid (Cho/Lip) ratio in liver VX2 tumor were increased and decreased to the level of ablated normal liver after tumor HIFU ablation. The changes of metabolites in tumor tissue observed in MRS were consistent with histopathologic changes. The findings suggest that MRS could differentiate the complete from residual tumor tissue and may be applied as an important, non-invasive marker for monitoring the thoroughness of HIFU ablation.

Materials and Methods

Animals

The animal experiments were in compliance with national and international regulations and approved by the Ethical Committee of Chongqing Medical University. Thirty-three New Zealand white rabbits (weight, 2.0–3.0 kg) were used in the study, which were purchased from the Animal Experimental Center of Chongqing Medical University (Chongqing, China). The VX2 cell line was derived from the rabbit VX2 squamous carcinoma, which was provided by the Institute of Ultrasonic Engineering in Medicine, Department of Biomedical Engineering, Chongqing Medical University.

Establishment of Tumor Model

Rabbits were inoculated subcutaneously with liver VX2 cells and showed tumor growth. When the size of the tumors reached 7 to 8 mm^3 in volume, the tumors were harvested, washed with normal saline, and then subdivided into small pieces of tissues of approximately 1 mm^3. The abdomen of the rabbit was routinely opened by median incision and the left or middle lobe of the liver was pricked to form a hole approximately 1 to 2 mm deep with ophthalmologic forceps. One piece of subdivided tissue was implanted into the hole. Bleeding points were stopped with gauze. The abdominal wall was sutured. The rabbits were administrated penicillin for 3 days after operation to prevent infection. Thirty-three rabbits were randomly divided into two groups, non-tumor group (normal control; n = 12) and tumor group (n = 21). After the establishment of rabbit liver tumor model, rabbits bearing VX2 tumors were randomly divided into two subgroups: tumor complete ablation (100% ablation of the tumor volume) and tumor partial ablation (80% ablation of the tumor volume) [7–9].

HIFU Treatment

Abdominal skin of each animal was shaved with 8% sodium sulfide 24 hours before the experiments. A model JC200 High-Intensity Focused Ultrasound Tumor Therapeutic System (Chongqing Haifu (HIFU) Technology Co Ltd, Chongqing, China) was used to ablate the whole mass of liver tumor in the complete ablation group and ablate 80% of tumor in volume in the partial ablation group. The strategy of treatment is HIFU ablation from "lines" to "slices", from "slices" to "volume", and from deep to shallow. B-mode ultrasonography (US) was used to target and monitor the whole therapeutic procedure HIFU treatment with parameters including interlamellar spacing of 3 mm, interline spacing of 5 mm, scanning speed of 3 mm/s, frequency set at 1.0 MHz, and acoustic power fixed at 180 W. The HIFU ablation procedure was in compliance with the guidance of the National Standard of China and has been described in detail previously [9].

Magnetic Resonance Imaging and MRS

Magnetic resonance imaging (MRI) was performed before and immediately after ablation using an MRI scanner (GE Signa Excite II 1.5 T) with an eight-channel cardiac phased array coil. The rabbits were subjected to the following MRI protocols: axial T1-weighted spin echo [repetition time (TR) of 170 ms, an echo time (TE) of 6.9 ms, a slice thickness of 3.0 mm, Field of view (FOV) = 180 × 180 mm, matrix = 256 × 192, and number of excitation = 3]; axial T2-weighted fast spin echo (TR = 3000 ms, TE = 85 ms, a slice thickness of 3.0 mm, 1.0-mm spacing, FOV = 180 × 180 mm, matrix = 256 × 192, and number of excitation = 6); MRS single voxel was performed by using point resolved spectroscopy sequences (TR = 3000 ms, TE = 35 ms, FOV = 240 × 240 mm, matrix = 1 × 1, and number of excitation = 8). MRS volume of interest was placed to cover the whole lesion based on lesion volume on T1WI and T2WI, and then outer volume saturation bands were placed around the volume of interest to avoid signal intensity contaminations. Peak assignments were given as follows: Cho at 3.22 ppm and lipids (Lip) at 1.3 ppm. The areas under the peaks are proportional to the metabolite concentrations, and Cho/Lip ratio was calculated.

Data Processing

After the acquisition process, raw data were post-processed with Saker software (GE) including the following steps: apodization, zero-filling, phase correction, baseline correction and the measurement of the area under the peak. The abscissa represents the magnitude of the chemical shift, and the magnetic resonance frequencies are expressed in "parts per million"; the ordinate represents the signal intensity of metabolites. The Cho-containing compound signal is detected as a single peak observed at 3.2 ppm; lipid signal is detected as a single peak observed at 1.3 ppm. The area under the peak was measured, and the Cho/Lip ratio was calculated.

Histology

Three liver samples of each group were collected before HIFU ablation as histologic studies, and other liver samples were collected

from rabbits' livers after HIFU and MRI processes. The samples were conserved in 10% formalin, and 5-μm-thick sequential sections were prepared for hematoxylin and eosin (H&E) staining to evaluate the basic histomorphology of the specimens.

Data Analysis

All data are expressed as the mean ± SD. Differences of the same group before and after HIFU ablation were evaluated by *t* test. The comparisons of the area under the Cho peak, area, and Cho/Lip ratio between groups were performed using a one-way analysis of variance followed by Fisher least significant difference post hoc test; $P < .05$ was considered as a statistically significant difference. Data were analyzed with the SPSS 13.0 statistical software package.

Results

Cho/Lip Ratio of Normal Liver Increases after Complete HIFU Ablation

Normal livers show normal T1-weighted images (T1WI) and T2-weighted images (T2WI) without mass in the left lobe of the liver (Figure 1, *A* and *B*). Histologic staining shows a normal liver architecture before HIFU (Figure 1*D*). Cho peak appeared at 3.2 ppm and Lip peak appeared at 1.3 ppm; the measured Cho/Lip ratio is 0.03 ± 0.00 (Figure 3). After complete HIFU ablation of normal liver, a lower intensity signal appeared on T1WI in the left lobe of normal liver, and T2WI shows a slightly high intensity signal (Figure 1, *E* and *F*). The MRS after HIFU shows a similar pattern to that before HIFU, and the Cho resonance is at 3.2 ppm with no significant changes in amplitude; however, the lipid resonance at 1.3 ppm increased, and Cho/Lip ratio after HIFU decreased to 0.02 ± 0.00 (Figures 1*G* and 3). The H&E-stained section shows lysed membranes, poorly delineated cells, pycnotic nuclei, nuclear fragmentation, and heavy staining of hepatocyte cytoplasm after HIFU ablation (Figure 1*H*).

Increased Cho Resonance and Cho/Lip Ratio of Liver VX2 Tumor

The rabbit VX2 tumor mass grows in the left or middle lobe of the liver 2 weeks after implantation, lesions appeared as slightly low intense nodules on T1WI (Figure 2, *A* and *I*) and hyperintense signal on T2WI (Figure 2, *B* and *J*). The Cho peak at 3.2 ppm was significantly increased to 3.16 ± 0.58, and the Cho/Lip ratio was significantly increased to 0.22 ± 0.03 in liver VX2 tumor in comparison with normal liver, $P < .001$ (Figures 1*C*, 2, *C* and *K*, and 3).

Decreased Cho Resonance and Cho/Lip Ratio of Liver VX2 Tumor after HIFU Ablation

Tumor lesion shows a slightly low intensity signal on T1WI and a slightly hyperintense signal on T2WI in both groups after complete HIFU ablation (Figure 2, *E* and *F*) and the partial HIFU ablation (Figure 2, *M* and *N*). The signals on T1WI did not show any changes after HIFU ablation in both groups (Figure 2, *A*, *E* and *I*, *M*). The signals on T2WI were decreased after HIFU ablation in both groups relative to those before ablation (Figure 2, *B*, *F* and *J*, *N*); however, the intensities of signal on T2WI after complete HIFU ablation did not show an obvious difference from those after partial HIFU ablation (Figure 2, *F* and *N*). The MRS after complete HIFU ablation shows a significant decrease of Cho resonance at 3.2 ppm to the level of normal liver after ablation; the amplitude of the lipid resonance at 1.3 ppm increased, and the Cho/Lip ratio decreased to 0.02 ± 0.00 (Figures 1*G*, 2*G*, and 3), $P < .001$. H&E staining shows complete coagulative necrosis with poorly delineated cells, lysed membranes, pycnotic nuclei, and nuclear fragmentation after complete HIFU ablation; viable tumor cells cannot be observed (Figure 2*H*). The intact tumor cells were shown before HIFU ablation (Figure 2, *D* and *L*). After partial HIFU ablation, the MRS shows a significant reduction of Cho resonance (Figure 2*O*), but the amplitude is still higher than normal liver or tumor after complete ablation (Figures 1*G* and 2*G*), $P < .001$; the Cho/Lip ratio of partial ablation was lower than that of complete ablation, $P < .001$ (Figure 3).

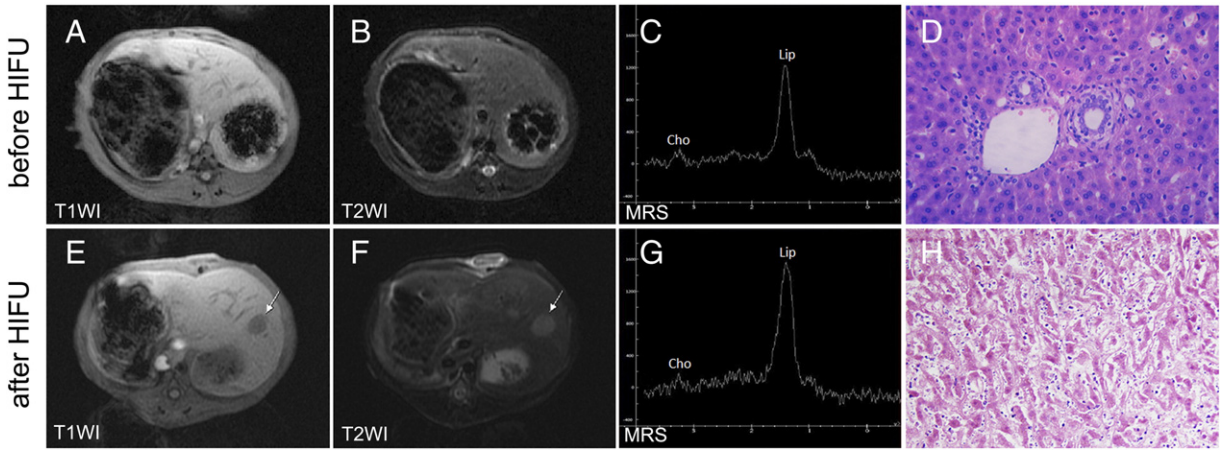

Figure 1. The MRI and MRS of normal liver before and after HIFU ablation. (A) T1WI of normal liver shows no mass in the left lobe of the liver. (B) T2WI of normal liver shows no mass in the left lobe of the liver. (C) MRS of normal liver shows that the Cho peak appeared at 3.2 ppm and Lip peak appeared at 1.3 ppm; the measured Cho/Lip ratio is 0.03 ± 0.00. (D) The H&E-stained section shows normal liver architecture before HIFU. (E) On T1WI after HIFU ablation, a lower intensity signal appeared in the left lobe of normal liver. (F) On T2WI after HIFU ablation, a slightly high intensity signal appeared in the left lobe of normal liver. The arrows indicate the ablated region on T1WI and T2WI. (G) The MRS after HIFU shows a similar pattern to that before HIFU, and the Cho resonance is at 3.2 ppm with no significant changes in amplitude; the lipid resonance at 1.3 ppm increased, and the Cho/Lip ratio after HIFU is 0.02 ± 0.00. (H) The H&E-stained section shows lysed membranes, poorly delineated cells, pycnotic nuclei, nuclear fragmentation, and heavy staining of hepatocyte cytoplasm after HIFU ablation.

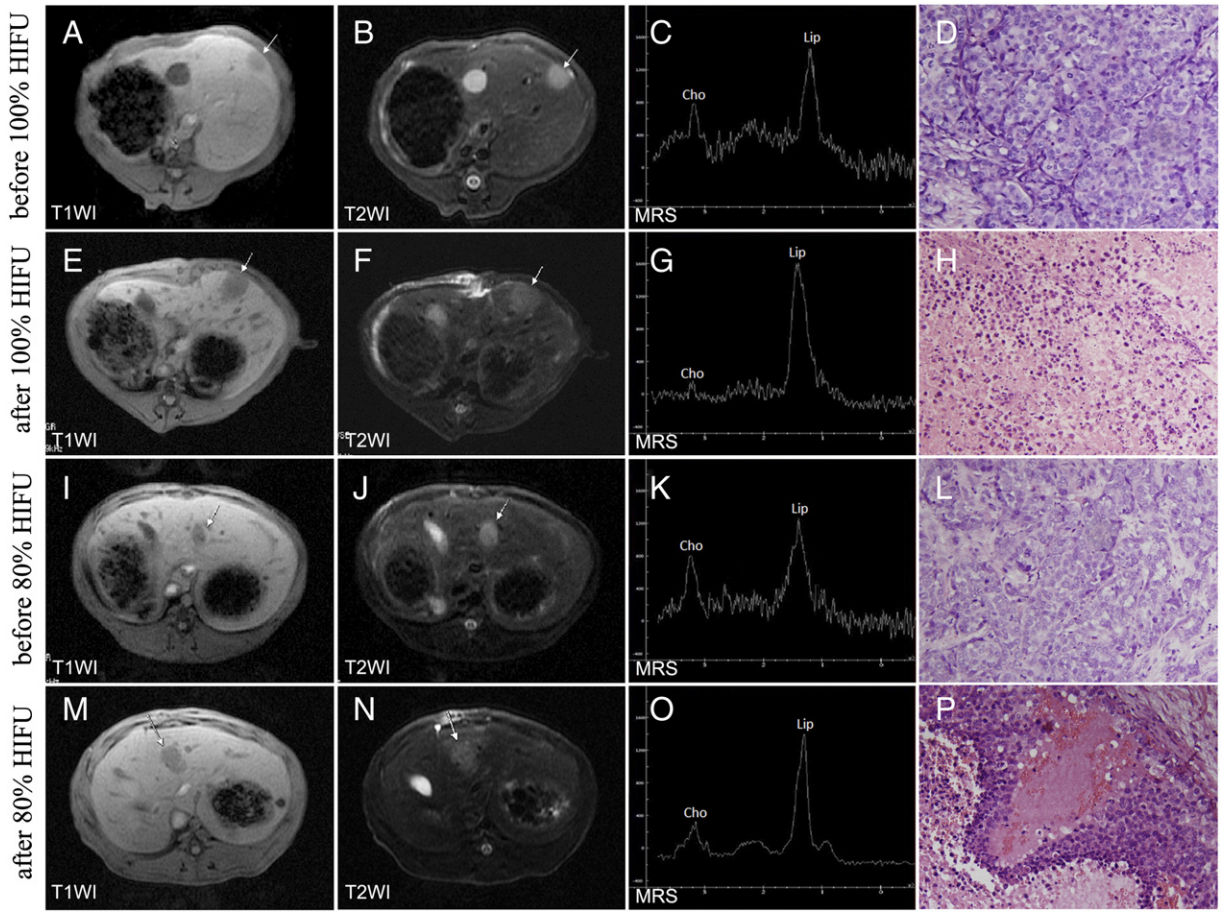

Figure 2. The MRI and MRS of liver VX2 tumor before and after complete and partial HIFU ablation. (A and I) Lesions of rabbit VX2 tumor were visible in the middle lobe of the liver 2 weeks after implantation, lesions appeared as slightly low intense nodules on T1WI images. (B and J) On T2WI, the lesions appeared hyperintense signals. (C and K) The Cho peak at 3.2 ppm is significantly increased in liver VX2 tumor (3.16 ± 0.58), and the Cho/Lip ratio is 0.22 ± 0.03. (D and L) The H&E-stained sections show untreated VX2 liver before HIFU. (E) On T1WI after complete HIFU ablation, the lesion shows a slightly low intensity signal. (F) On T2WI after complete HIFU ablation, the lesion shows a slightly hyperintense signal. (G) The MRS after complete HIFU ablation shows a significant decrease in Cho resonance at 3.2 ppm with no significant changes in amplitude; the amplitude of the lipid resonance at 1.3 ppm increased, and the Cho/Lip ratio after HIFU is 0.02 ± 0.00. (H) The H&E-stained section shows poorly delineated cells, lysed membranes, pycnotic nuclei, and nuclear fragmentation after complete HIFU ablation; viable tumor cells cannot be observed. (M) On T1WI after partial HIFU ablation, the lesion shows a slightly low intensity signal. (N) On T2WI after partial HIFU ablation, the lesion shows a slightly hyperintense signal. (O) The MRS after partial HIFU ablation shows a reduction in Cho resonance, but the amplitude is still higher than normal liver or tumor after complete ablation. (P) The H&E-stained section shows coagulative necrosis in the region of ablation, but viable tumor cells can be found adjacent to the necrosis. The arrows indicate the tumor mass on T1WI and T2WI.

Histology shows coagulative necrosis in the region of ablation, but viable tumor cells can be found adjacent to the necrosis (Figure 2*P*).

Discussion

HIFU has been applied to ablate solid malignant tumor with a well-defined volume. It has the advantages of non-invasion, non-ionization, and fewer complications after treatment in comparison to conventional surgery, radiotherapy, and chemotherapy. However, tumor relapse due to incomplete ablation still remains a clinical challenge that calls for the imaging modalities to identify the completeness of tumor necrosis. Recently, MRI or US is generally used to guide and monitor HIFU ablation, and guidance of HIFU by US in China is preferable, because of its low cost. During the HIFU ablation procedure, hyperechoic changes on grayscale ultrasound images obtained after each exposure are used to evaluate the extent of the area ablated on each slice [10–13]. However, the appearance of hyperechoic changes does not always mean complete tumor necrosis [14–17]. In addition, conventional MRI and contrast-enhanced (CE) MRI were used to evaluate the changes of tumor size and signal intensity and also to detect the tumor necrosis in primary hepatic carcinoma after HIFU ablation for follow-up [18]. However, CE MRI has been unsuccessful to early detect tumor residual so far, due to the similar nonspecific contrast enhancement in the periphery area of the ablation, which may confuse residual tumor with benign peri-ablational hyperemic tissue or reactive granulation tissue because of increased capillary permeability and therefore increase the passive distribution of contrast reagents [19,20]. Likewise, the hepatic carcinoma reoccurrences were detected at the margin of the treated lesions 3 months after HIFU ablation due to cancer residual, which means CE MRI failed to detect the tumor residual early after HIFU ablation [18]. The recent detection of tumor residual and relapse depends on long-term periodical follow-up with MRI after treatment,

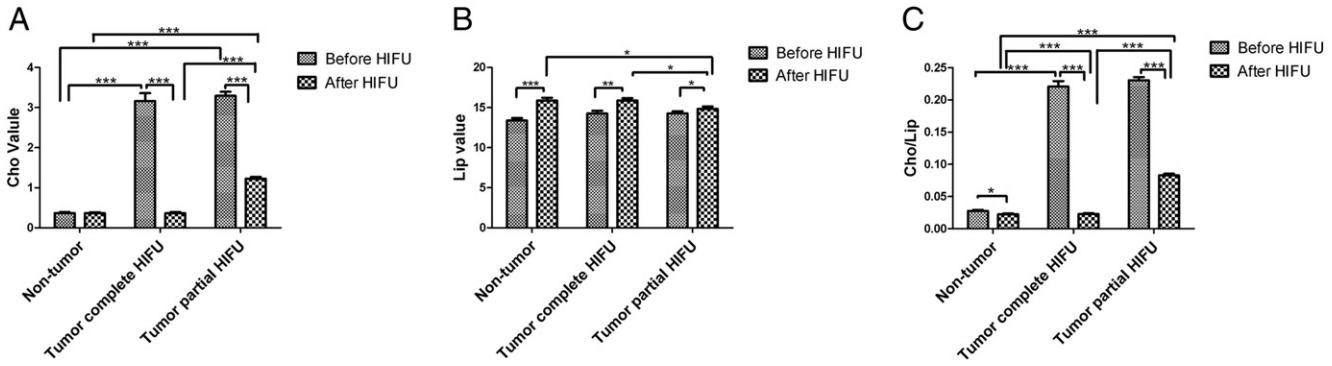

Figure 3. Comparison of Cho, Lip, and Cho/Lip ratio in normal liver and liver VX2 tumor before and after HIFU ablation. (A) Cho value in non-tumor, tumor complete HIFU, and tumor partial HIFU groups before and after HIFU ablation. (B) Lip value in non-tumor, tumor complete HIFU, and tumor partial HIFU groups before and after HIFU ablation. (C) Cho/Lip ratio in non-tumor, tumor complete HIFU, and tumor partial HIFU groups before and after HIFU ablation. ***$P < .001$, **$P < .01$, and *$P < .05$.

which may leave a broad time window to keep tumor progression. Therefore, it is necessary to early evaluate the adequacy of tumor lesion necrosis after HIFU ablation with another imaging modality. We tried to access the completeness of liver tumor necrosis early after HIFU ablation from a functional perspective. Therefore, we introduced MRS into the assessment of HIFU ablation on liver tumor to see whether MRS can show the difference of the metabolites in tumors after complete and partial HIFU ablation.

MRS is an analytical method that is used to identify and quantify the metabolites in human tissues. It differs from conventional MRI in that the spectra provide physiological and chemical information instead of anatomy. MRS has been used for cancer diagnosis, treatment monitoring, and patient follow-up [6,21].

The Cho peak is assigned at 3.2 ppm and represents the sum of Cho and Cho-containing compounds (e.g., Cho, phosphocholine, and glycerophosphocholine). Cho is a marker for cellular membrane turnover (phospholipid synthesis and degradation) that reflects cell-membrane metabolism. Its increase has been attributed to increased biosynthesis of membrane phospholipids and therefore cellular proliferation. Abnormal levels of Cho compounds were typically found in more active tumor masses [22]. Viable tumors consist of rapidly proliferating cells, causing a high Cho peak, whereas necrotic tumors have decreased cellularity, causing the Cho peak to diminish. Lipid compounds peak at 0.9 to 1.4 ppm that represent cell necrosis or membrane breakdown that may precede necrosis. In *in vivo* proton MRS, the evaluation of Cho levels was used to differentiate benign and malignant tumors [23].

In this study, we investigated the characterization of MRS before and early after HIFU treatment in VX2 liver cancer tissue and normal liver. Normal liver did not show any significant difference of Cho peak after HIFU treatment; however, the lipid peak increased, which resulted from liver necrosis, and the Cho/Lip ratio of normal liver after HIFU was significantly decreased in comparison to that in normal liver. The Cho of VX2 liver cancer tissue was significantly higher than that of normal livers, which is consistent with the previous study [6], and the Cho significantly decreased in both complete ablation group and partial ablation group after treatment. The Cho in complete ablation group did not show any difference with normal liver; however, the Cho in the partial ablation group was higher than that in normal liver before or after HIFU treatment due to the residual part of tumors, which was confirmed by pathologic examinations. The Cho and Cho/Lip values show a significant difference between partial ablation group and complete ablation group after HIFU treatment, so MRS may have the potential to distinguish residual portions of liver tumor from necrosis and perform additional HIFU ablation on residual portions, for future clinical monitoring of HIFU ablation, and the Cho and Cho/Lip of normal liver tissue close to the lesion can be used as a self-reference.

In conclusion, MRS may be used as a complement to conventional MRI after HIFU treatment to provide some information about the biochemical changes for immediately identifying the tissue coagulation and tumor residual during MRI-guided HIFU treatment or early evaluation of HIFU treatment.

References

[1] Kennedy JE, Wu F, ter Haar GR, Gleeson FV, Phillips RR, Middleton MR, and Cranston D (2004). High-intensity focused ultrasound for the treatment of liver tumours. *Ultrasonics* **42**(1–9), 931–935.

[2] Wu F, Chen WZ, Bai J, Zou JZ, Wang ZL, Zhu H, and Wang ZB (2002). Tumor vessel destruction resulting from high-intensity focused ultrasound in patients with solid malignancies. *Ultrasound Med Biol* **28**(4), 535–542.

[3] Ng KK, Poon RT, Chan SC, Chok KS, Cheung TT, Tung H, Chu F, Tso WK, Yu WC, and Lo CM, et al (2011). High-intensity focused ultrasound for hepatocellular carcinoma: a single-center experience. *Ann Surg* **253**(5), 981–987.

[4] Taylor JS, Langston JW, Reddick WE, Kingsley PB, Ogg RJ, Pui MH, Kun LE, Jenkins III JJ, Chen G, and Ochs JJ, et al (1996). Clinical value of proton magnetic resonance spectroscopy for differentiating recurrent or residual brain tumor from delayed cerebral necrosis. *Int J Radiat Oncol Biol Phys* **36**(5), 1251–1261.

[5] Kurhanewicz J, Vigneron DB, and Nelson SJ (2000). Three-dimensional magnetic resonance spectroscopic imaging of brain and prostate cancer. *Neoplasia* **2**(1–2), 166–189.

[6] Kuo YT, Li CW, Chen CY, Jao J, Wu DK, and Liu GC (2004). In vivo proton magnetic resonance spectroscopy of large focal hepatic lesions and metabolite change of hepatocellular carcinoma before and after transcatheter arterial chemoembolization using 3.0-T MR scanner. *J Magn Reson Imaging* **19**(5), 598–604.

[7] Furusawa Y, Zhao QL, Hassan MA, Tabuchi Y, Takasaki I, Wada S, and Kondo T (2010). Ultrasound-induced apoptosis in the presence of Sonazoid and associated alterations in gene expression levels: a possible therapeutic application. *Cancer Lett* **288**(1), 107–115.

[8] Orsi F, Arnone P, Chen W, and Zhang L (2010). High intensity focused ultrasound ablation: a new therapeutic option for solid tumors. *J Cancer Res Ther* **6**(4), 414–420.

[9] Zhou SJ, Li SW, Wang JJ, Liu ZJ, Yin GB, Gong JP, and Liu CA (2012). High-intensity focused ultrasound combined with herpes simplex virus

thymidine kinase gene-loaded ultrasound-targeted microbubbles improved the survival of rabbits with VX_2 liver tumor. *J Gene Med* **14**(9–10), 570–579.

[10] Wu F, Wang ZB, Chen WZ, Wang W, Gui Y, Zhang M, Zheng G, Zhou Y, Xu G, and Li M, et al (2004). High-intensity focused ultrasound for the treatment of liver tumours. Extracorporeal high intensity focused ultrasound ablation in the treatment of 1038 patients with solid carcinomas in China: an overview. *Ultrason Sonochem* **11**(3-4), 149–154.

[11] Wu F, Wang ZB, Chen WZ, Zhu H, Bai J, Zou JZ, Li KQ, Jin CB, Xie FL, and Su HB (2004). Extracorporeal high intensity focused ultrasound ablation in the treatment of patients with large hepatocellular carcinoma. *Ann Surg Oncol* **11**(12), 1061–1069.

[12] Wu F, Wang ZB, Chen WZ, Zou JZ, Bai J, Zhu H, Li KQ, Jin CB, Xie FL, and Su HB (2005). Advanced hepatocellular carcinoma: treatment with high-intensity focused ultrasound ablation combined with transcatheter arterial embolization. *Radiology* **235**(2), 659–667.

[13] Illing RO, Kennedy JE, Wu F, ter Haar GR, Protheroe AS, Friend PJ, Gleeson FV, Cranston DW, Phillips RR, and Middleton MR (2005). The safety and feasibility of extracorporeal high-intensity focused ultrasound (HIFU) for the treatment of liver and kidney tumours in a Western population. *Br J Cancer* **93**(8), 890–895.

[14] Vaezy S, Shi X, Martin RW, Chi E, Nelson PI, Bailey MR, and Crum LA (2001). Real-time visualization of high-intensity focused ultrasound treatment using ultrasound imaging. *Ultrasound Med Biol* **27**(1), 33–42.

[15] Rabkin BA, Zderic V, and Vaezy S (2005). Hyperecho in ultrasound images of HIFU therapy: involvement of cavitation. *Ultrasound Med Biol* **31**(7), 947–956.

[16] Rabkin BA, Zderic V, Crum LA, and Vaezy S (2006). Biological and physical mechanisms of HIFU-induced hyperecho in ultrasound images. *Ultrasound Med Biol* **32**(11), 1721–1729.

[17] Yu T and Xu C (2008). Hyperecho as the indicator of tissue necrosis during microbubble-assisted high intensity focused ultrasound: sensitivity, specificity and predictive value. *Ultrasound Med Biol* **34**(8), 1343–1347.

[18] Zhang Y, Zhao J, Guo D, Zhong W, and Ran L (2011). Evaluation of short-term response of high intensity focused ultrasound ablation for primary hepatic carcinoma: utility of contrast-enhanced MRI and diffusion-weighted imaging. *Eur J Radiol* **79**(3), 347–352.

[19] Vossen JA, Buijs M, and Kamel IR (2006). Assessment of tumor response on MR imaging after locoregional therapy. *Tech Vasc Interv Radiol* **9**(3), 125–132.

[20] Rowland IJ, Rivens I, Chen L, Lebozer CH, Collins DJ, ter Haar GR, and Leach MO (1997). MRI study of hepatic tumours following high intensity focused ultrasound surgery. *Br J Radiol* **70**(2), 144–153.

[21] Chen CY, Li CW, Kuo YT, Jaw TS, Wu DK, Jao JC, Hsu JS, and Liu GC (2006). Early response of hepatocellular carcinoma to transcatheter arterial chemoembolization: choline levels and MR diffusion constants—initial experience. *Radiology* **239**(2), 448–456.

[22] Shin HJ, Baek HM, Cha JH, and Kim HH (2012). Evaluation of breast cancer using proton mr spectroscopy: total choline peak integral and signal-to-noise ratio as prognostic indicators. *AJR Am J Roentgenol* **198**(5), W488–W497.

[23] Doganay S, Altinok T, Alkan A, Kahraman B, and Karakas HM (2011). The role of MRS in the differentiation of benign and malignant soft tissue and bone tumors. *Eur J Radiol* **79**(2), e33–e37.